LOAD TESTS ON THE NEW RAILWAY BRIDGES AT TUNYOGMATOLCS AND BÁNRÉVE

A. SZITTNER, M. KÁLLÓ and L. KÖRÖNDI

Department of Steel Structures
Technical University, H–1521 Budapest

Received: January 20, 1992.

Abstract

In this paper, the results of load tests performed on two railway bridges opened to traffic recently are demonstrated. In the course of static measurement, the deflection of the bridge and the stresses in selected points were measured. Dynamic measurements comprised natural frequencies, dynamic factor and dynamic excess. The measurement results obtained were compared with the calculated deflections and stresses. Comparison of model test results for the Simontornya bridge in the design stage and measurement results for the structurally similar Bánréve bridge is of special interest.

Keywords: static, dynamic, load test, railway bridge.

The Department of Steel Structures at the Technical University of Budapest performed the examination of the above bridges in Hungary prior to opening them to traffic.

The Railway Bridge over the River Szamos at Tunyogmatolcs

The bridge is a continuous, welded truss girder open above with cross-girder distances of 5750 mm and a span layout of 4×46 m. The structure was built with box-girder profiles and HSFG field joints *(Fig. 1)*. The floor structure was constructed with two stringers at a distance of 1500 mm from each other and a continuous flange plate above, which is connected also to the flange-plate of the cross girder. The upper flange is an orthotropic plate. The floor structure works together with the bottom chord of the main girder through the joint at the cross-girders and through the built-in brake structures. This contribution was not taken into consideration regarding the main girder, but the floor girders were dimensioned for the overloading from the contribution effect. The tie-plates (Geo plates) were bonded to the flange of the stringers.

The bridge was designed by the planning bureau UVATERV, manufactured and assembled by the factory GANZ-MÁVAG. The field erecting in the axis of the bridge took place on the embankments, and then the whole bridge was pulled longitudinally into its ultimate place.

The task of the Department was:

examination of the structural behaviour during the erection,

completing the static and the dynamic load test.

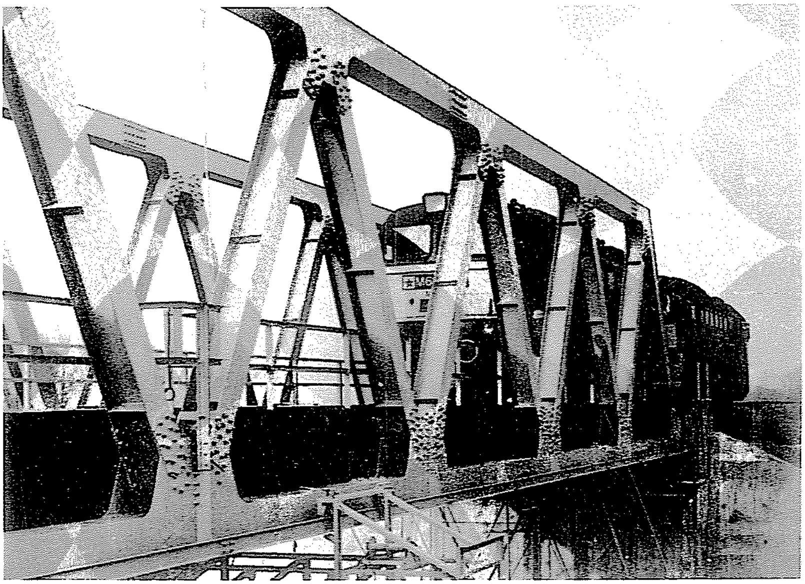

Fig. 1. Main girder of the bridge at Tunyogmatolcs, and the locomotives used for the load test.

Examination of the Structural Behaviour during Erection

In the course of the pull-in operation, the most unfavourable situation from force theory point of view was developed when the front part of the bridge was functioning as a cantilever in 7 frame-joint length. This state was controlled by disassembling the supporting piles before starting the pull-in operation. Before the disassembling of piles, measuring stations were developed in the middle of the bottom and upper chords at the support for strain-gage measurement of Pfender-type. After disassembling the piles, the following average stresses were measured:

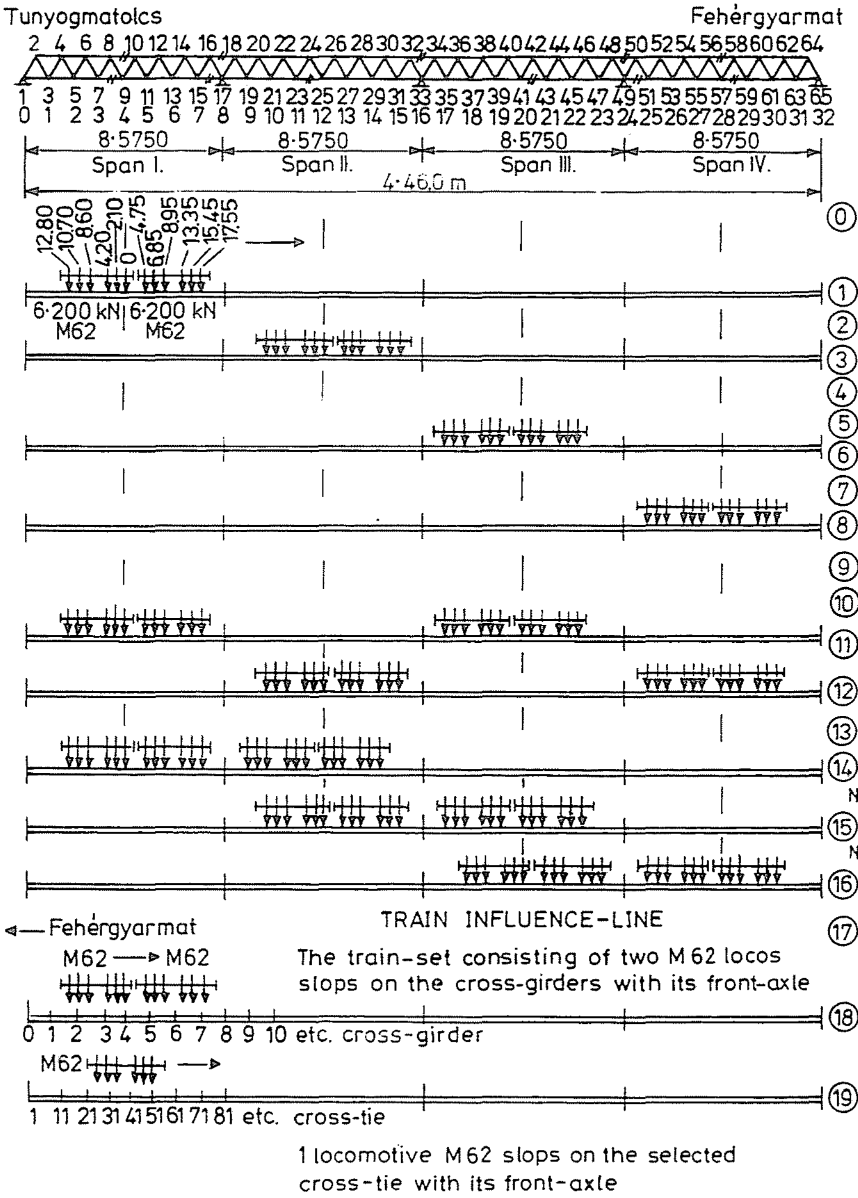

Fig. 2. Load positions applied with the load test.

Table 1

Railway Bridge at Tunyogmatolcs

Comparison between the measured (M) and calculated (C) stresses in the course of static load test (kN/cm^2)

Number of load position	Loaded span Total load	Span IV 7–9 A 232.4cm^2	Span IV 8–10 A 297.6cm^2	Support III-IV 15–17 A 166cm^2	Support III-IV 16–18 A 215.2cm^2	Span III 23–25 A 215.2cm^2	Support II-III 32–34 A 193.3cm^2
1	Span I	-0.042	0.037	-0.126	0.103	0.195	-0.623
	Σ C	-0.0427	0.037	-0.126	0.103	0.195	-0.623
3	Span II	0.211	-0.181	0.608	-0.500	-0.946	3.028
	C	0.211	-0.181	0.608	-0.500	-0.946	3.028
	M	0.06	0.92	0.43	-0.69	-0.19	3.16
	M	0.08	-0.36	0.43	-0.72	-0.41	3.23
6	Span III	-1.029	0.908	-3.089	2.542	4.244	3.028
	Σ C	-1.029	0.908	-3.089	2.542	4.244	3.028
	M	-0.53	0.92	-2.10	2.24	2.83	2.07
	M	-0.50	0.96	-2.18	2.30	3.00	2.35
8	Span IV	5.139	-4.017	-1.681	3.083	-7.483	-0.623
	Σ C	5.139	-4.017	-1.681	3.083	-7.483	-0.623
	M	3.32	4.01	-2.41	2.70	-0.84	-0.37
	M	3.30	3.78	-2.47	2.73	-0.91	-0.25
11	Span I	-0.042	0.037	-0.126	0.103	0.195	-0.623
	Span II	-1.029	0.908	-3.089	2.542	4.244	3.028
	Σ C	-1.071	0.945	-3.215	2.645	4.439	2.405
	M	-0.52	1.30	-2.14	2.69	2.91	1.80
	M	-0.50	1.11	-2.27	2.67	2.88	1.78
12	Span II	0.211	-0.181	0.608	-0.500	-0.946	3.028
	Span IV	5.139	-4.017	-1.681	3.083	-1.483	-0.623
	Σ C	5.350	-4.198	-1.073	2.583	-2.429	2.405
	M	3.30	4.16	-1.95	2.00	-1.18	1.57
	M	3.32	4.017		2.02	-1.29	0.171
14	Span I	-0.0142	0.037	-0.126	0.103	0.195	-0.623
	Span II	0.191	-0.170	0.573	-0.471	-0.91	2.848
	Σ C	0.149	-0.133	0.447	-0.368	-0.696	2.225
	M	0.04	0.27	0.34	-0.41	-0.25	2.01
	M	0.04	0.15	0.28	-0.34	-0.18	2.00
15	Span II	0.211	-0.181	0.608	-0.500	-0.946	3.028
	Span III	-1.029	0.908	-3.089	2,542	4.244	3.028
	Σ C	-0.818	0.727	-2.481	-2.042	3.289	6.056
	M	-0.40	0.98	-1.61	1.88	2.29	5.47
	M	-0.35	-0.89	-1.74	2.03	2.47	5.47
16	Span III	1.094	0.967	-3.283	-2.702	4.345	2.848
	Span IV	5.139	-4.017	-1.681	3.083	-1.483	-0.623
	Σ C	4.045	-3.050	-4.967	5.785	2.862	2.225
	M	2.79	-2.99	-4.85	4.73	2.09	1.79
	M	2.70	-2.89	5.06	4.65	2.17	2.53

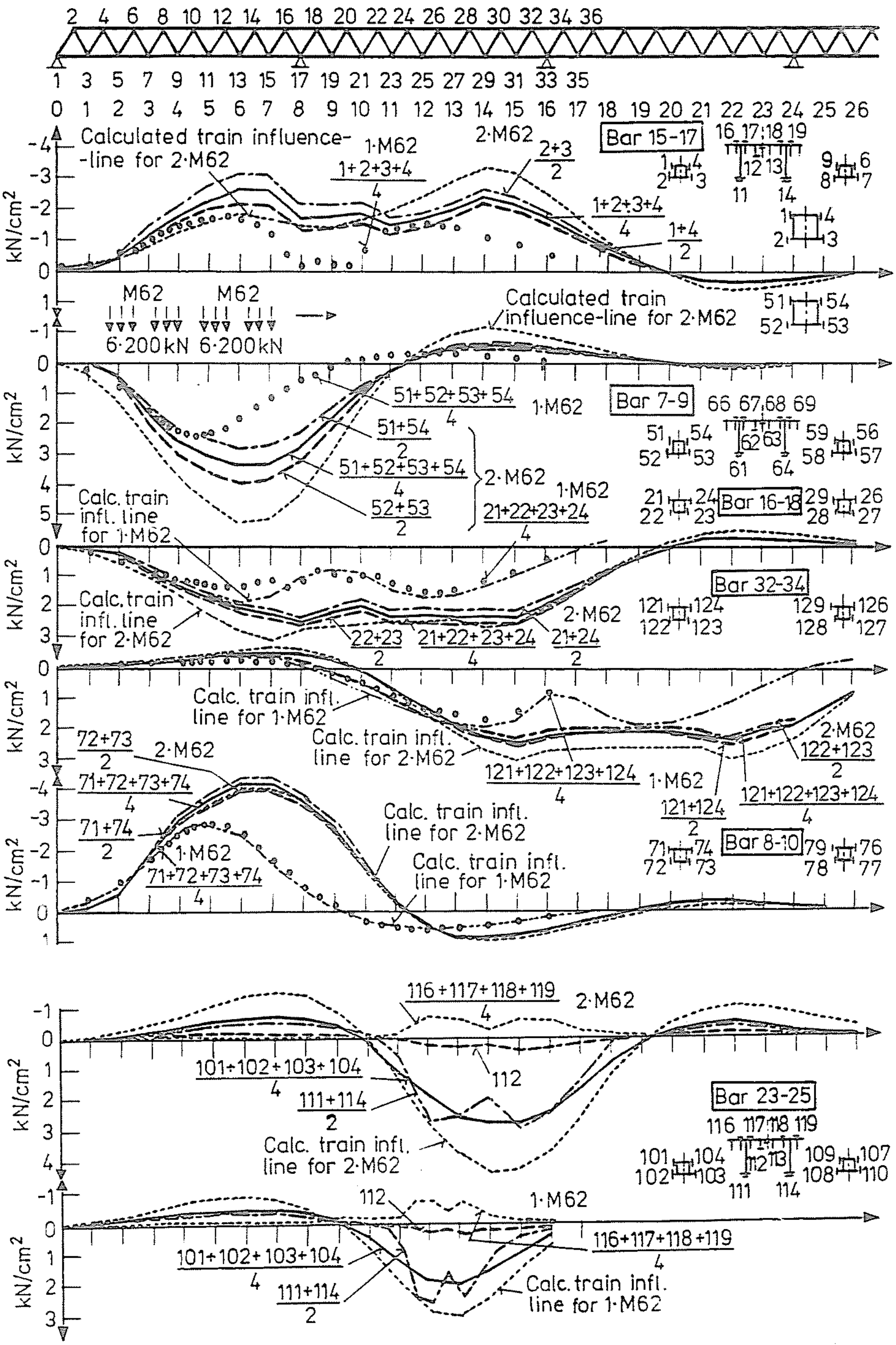

Fig. 3. Train influence lines of the stresses measured in the chords

- on the upper chord bar No. 50-52, with a nearly uniform stress distribution σ=14.32 kN/cm^2,
- on the bottom chord bar No. 51-53,
  on the bottom exterior fibre: σ=–8.57 kN/cm^2,
  on the upper exterior fibre: σ=–5.25 kN/cm^2,
- in the same section of the stringer,
  on the bottom flange plate: σ=–5.99 kN/cm^2,
  on the upper flange plate: σ=–0.38 kN/cm^2.

The deflection of the cantilever-ends were 236 mm and 214 mm, respectively. With the satisfying results, the pulling-in operation took place according to the plans.

Static load test

The static load tests covered
 shape measurement,
 measurement of deformations and
 stress measurements.

The load test took place using 2×2 pieces of M62 locomotives having a mass of 120 t each. As a first step, the locomotives were positioned to the most unfavourable place with respect to the mains, later train influence lines were recorded first for the mains, using 2 locomotives (the front axle positioned above each cross-girder, successively), then for the stringer, using one locomotive (front axle placed above each tie, successively), see *Fig. 2.*

By the shape measurement, the shape of the bridge was recorded prior to and after the static load test.

The maximum value of residual deformation of the main girders proved to be 3.3 mm and 2.3 mm, respectively. The deflection measured under the influence of train load was about 80 % of that obtained by calculation.

Stress measurement was performed in the vicinity of the positive and negative maxima on the bottom and upper chords of the main girder, as well as on the floor structures by using Kyowa-type foil resistance strain gages of 5 mm base bonded on with an adhesive of cyanoacrylate. The measuring system was composed of Hottinger-type units with a connection to the measuring stations ensured by a personal computer, which also provided the control of switch-over to the measuring points and that of data acquisition process.

The measured and calculated results related to the most unfavourable static load positions are shown in *Table 1.* Measured stresses are smaller then the calculated ones with the exception of those in the bottom chord is greater with the bottom chords (cc 30 %). With the bar 15-17, there is a considerable deviation at one of the load positions, however, this deviation will occur with the train influence line to be dealt with later on.

The results obtained with the train influence lines are in full harmony with those described above *(Fig. 3)*. Thus, e.g. on the bottom chord 7-9, the calculated and measured train influence lines are conform with a train of two locomotives taken as a basis, however, the measured stress is lower by about 30 % than the calculated one. The forms of the measured and calculated train influence lines of stresses in the bar 15-17 do not agree with each other. According to the measurements, the maximal stresses will occur when the train is moving within the span No.1, while the train influence line processed on the basis of the calculated bar force influence line will yield the maximal value within span No.2. The measured stress influence lines of the upper chords No.16-18, 32-34 and 8-10 are in good agreement with the calculated ones with both the one and the two locomotive train. The comparison of the calculated and measured stresses on the bottom chord 23-25, or on the stringer contained in this section can be seen in *Fig. 3*.

Dynamic Measurements

In the course of dynamic measurements, the following values were measured:

- natural frequencies of the unloaded bridge in the horizontal and the vertical plane,
- motion of tie-plates,
- compression of plastic layers under tie-plates,
- midspan deflections,
- midspan horizontal vibration.

The measured quantities were recorded by instrumentation tape-recorder and an 8 channel strip chart recorder at the same time. Recorded data were processed later by computer, via A/D conversion. Digital signals were frequency-analyzed, scaled, filtered, according to the needs of processing requirements.

- In *Fig. 4*, the power spectrum of free oscillations, i.e. natural frequencies in vertical and horizontal directions,
- in *Fig. 5* the compression diagrams of the plastic-mortar under tie-plates and that of the full rail-plate,
- in *Fig. 6* the horizontal transverse oscillations of the fourth and third spans, excited by moving load,
- in *Fig. 7* the deflection recorded in the fourth span,

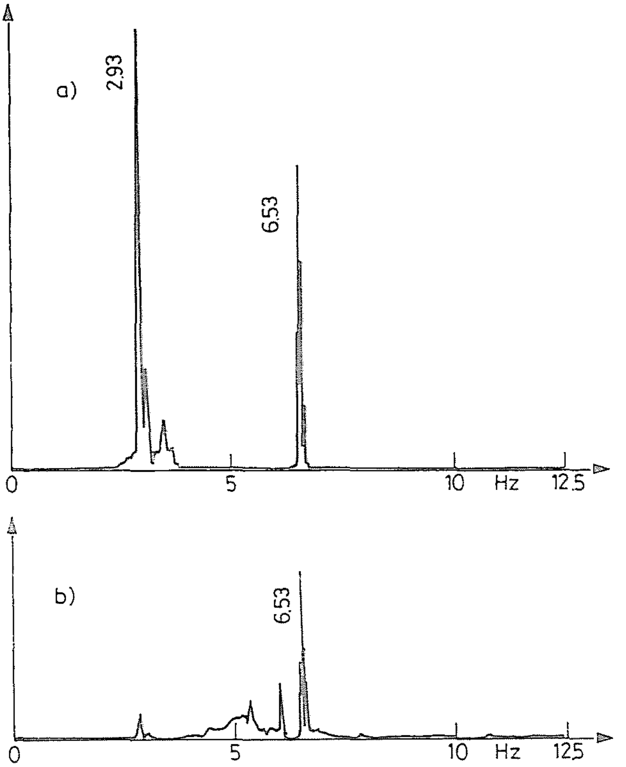

Fig. 4. Power spectrum of natural frequency measured in a) horizontal, and b) vertical directions

- in *Fig. 8* the stresses measured by the two gages located on the bottom chord 7-9 in the case of quick train motion can be seen.

Bridge over the River Sajó at Bánréve

The bridge is a simple-supported, welded, trussed closed bridge with a span of 66 m and an inclined portal frame, as well as a clearance gage for electric traction. The horizontal distance of the joints is 8250 mm which is reduced by setting in two intermediate cross girders. The distance between the stringers is 1500 mm. The stringers and cross girders are of the same height, their upper flange plates are connected in a single, cross-shaped plate of 40 mm in thickness. The ties are fastened to the stringers in both longitudinal and transversal directions.

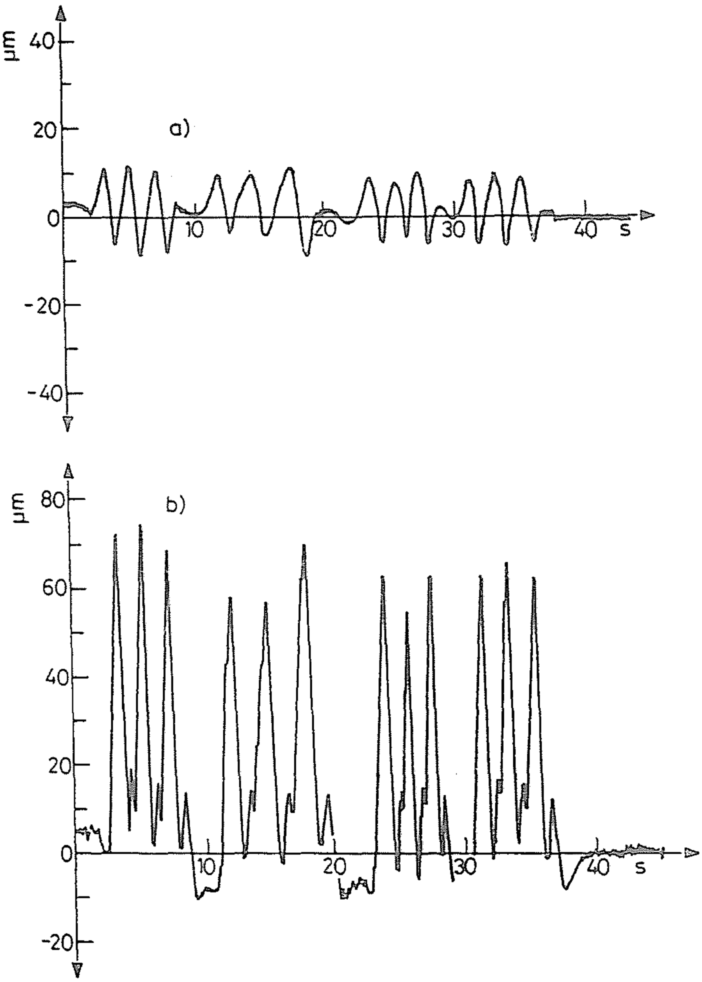

Fig. 5. a) Compression of plastic mortar under the tie plates; b) total compression of the whole tie plates

The profiles of the welded, trussed main girder bars are of I-shape, and the inner flange plates of the chords at the joints are transduced to the flange plates of the truss members in an arched form (*Fig. 9*). The joints are riveted with the exception of the upper wind brace which is bolted.

The main girders and the floor beams are connected together rigidly. With calculations of the main girder, this contribution was not taken into consideration, however, the floor girders were dimensioned for the addi-

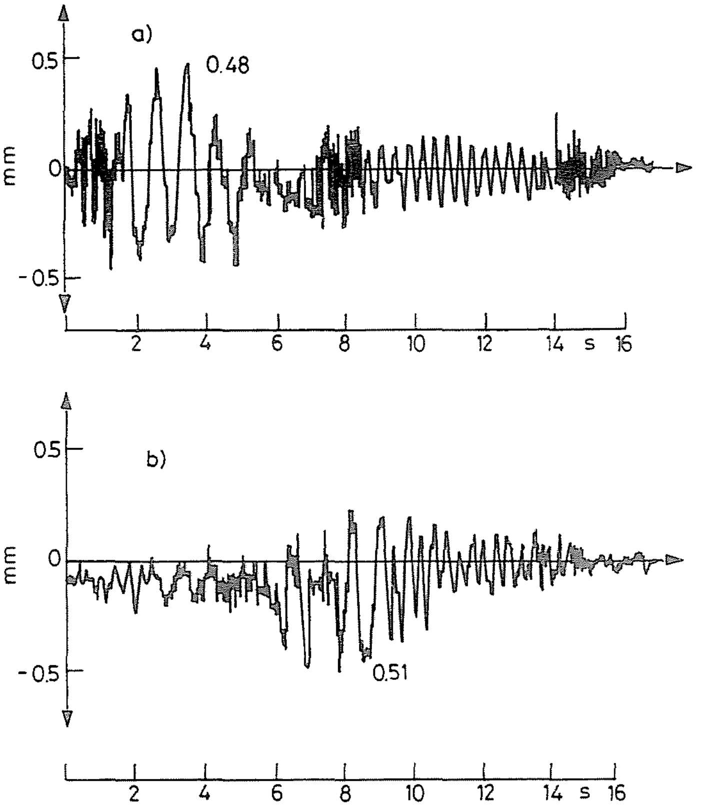

Fig. 6. Horizontal, lateral oscillation a) in the fourth span, and b) in the third span

tional load resulting from the contribution between the structural elements mentioned above.

The bridge was mounted fully on the embankment, and afterwards it was pulled in – first in longitudinal, then in transverse direction – into the place of the former bridge.

The bridge was designed by the planning bureau UVATERV, while it was implemented by the MÁV (Hungarian State Railways).

The investigated bridge structure is similar to that of the new bridge designed for service over the river Sió at Simontornya, the plans of which drafted also by the UVATERV were checked by the Department of Steel Structures earlier. The process of checking took place by calculation, and – for developing the joints of the truss and determination their static behaviour – by a so-called 'hybrid' method with a photoelastic model, in

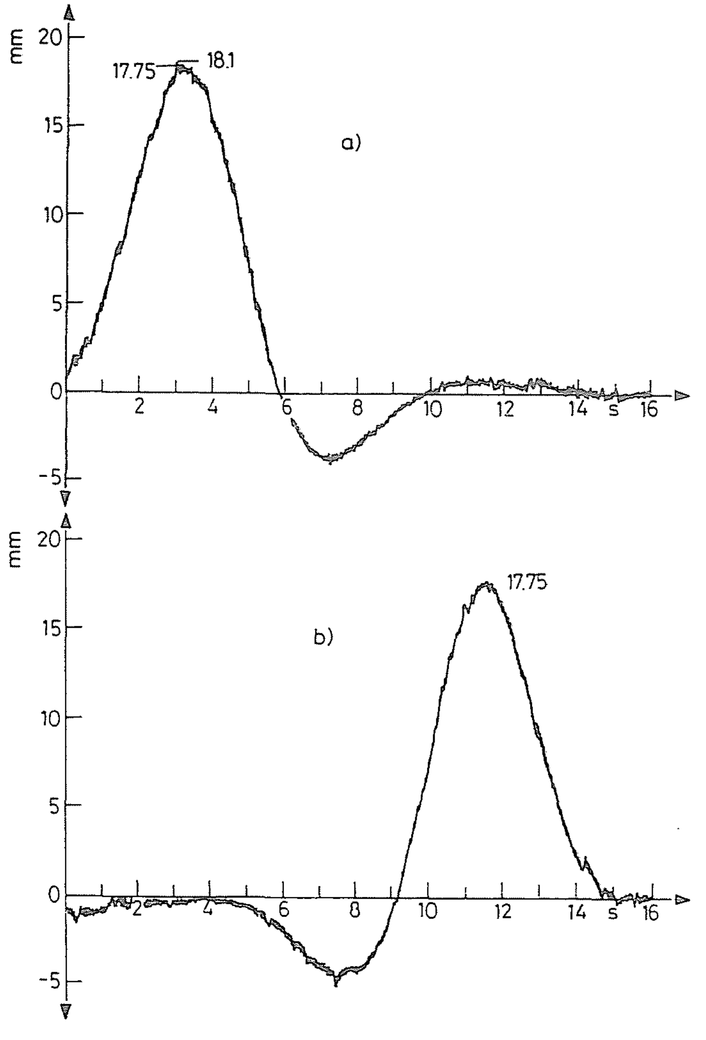

Fig. 7. Deflection in the middle of the fourth span during the running forward and reverse

which the stress distribution was determined by resistance strain gages on the curved flange plates and on the web in the places of stress concentration pointed out by photoelastic methods (*Fig. 10*).

Using these results, the measuring points were selected prior to the load-test of the bridge, and afterwards the measurement results obtained in the course of loadtests could be compared with those obtained during model experiments.

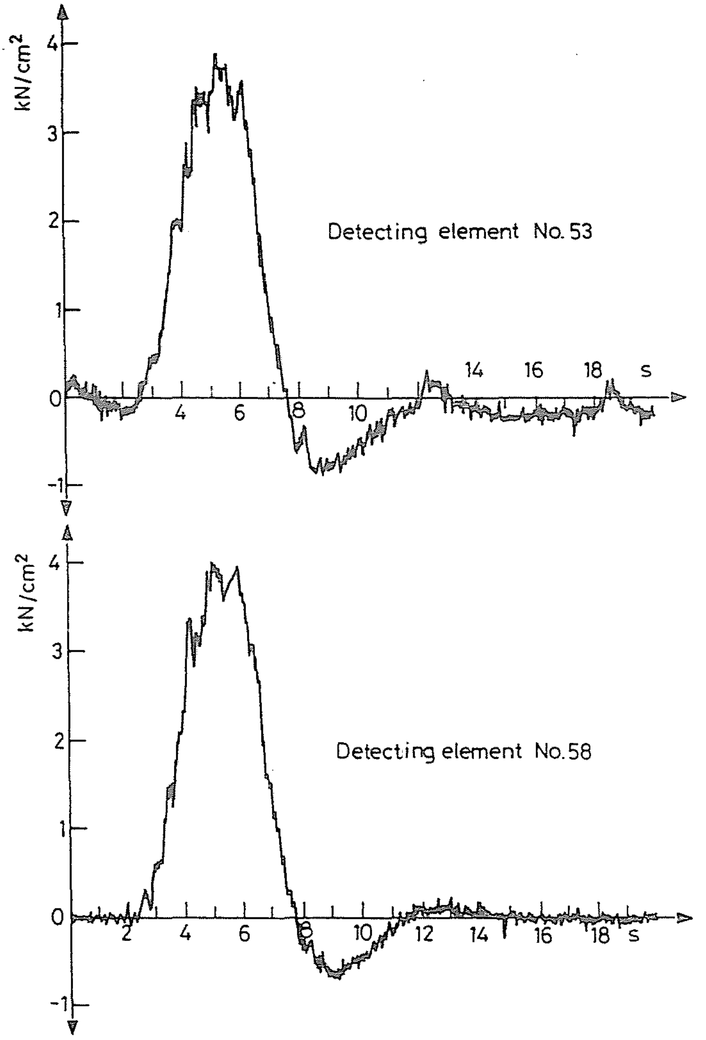

Fig. 8. Stresses measured in the bottom chord bar No. 7-9 during fast running

Due to the extremely short stop peace-time static load tests and dynamic tests were performed.

For the load tests, 3 M62-type locomotives coupled to each other were stopped at the most unfavourable position for joint No.8.(the main point of the upper chord bar No.7-7'). During the record of the train influence line, also three coupled locomotives were moved, while the dynamic load test took place with 3 coupled locomotives, and then with a single locomotive.

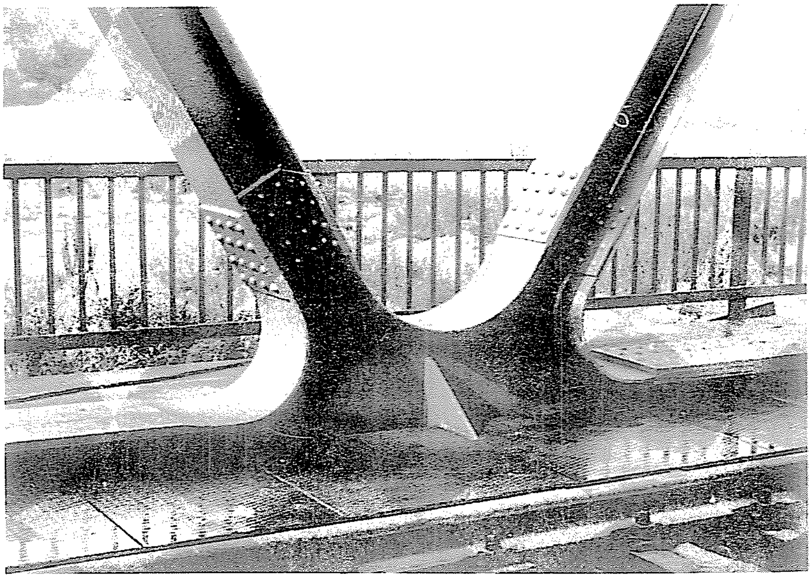

Fig. 9. One of the joints of the railway bridge at Bánréve

Static Load test

In the course of the load test, the midspan deflection and the stresses or strains, respectively, were measured in the characteristic points. In each case – taking the significant subsidiary stresses into consideration – the normal and bending components of the stresses acting on the cross-section were calculated from the measurement results, and then the measured stresses were compared – where it was possible – with the stresses calculated on the basis of the load applied.

The resistance strain gages were positioned in the characteristic cross-sections of the main girders and the stringers, on the arched flange plate at joint No.8., on the sections of the tangents subtending an angle of 0°, 20°, 40° and 60°, with respect to the results of our earlier model experiments. On the sections with tangent-angle 20° and 40°, a rosette was bonded on at a distance of about 20 mm from the web-to-flange fillet weld on both sides of the web. To determine the effect of the deflection caused by horizontal forces, strain gages were positioned on the edge of each flange plate in three sections of the end cross-girder No.0. (*Fig. 11*).

The measuring system applied here was the same as that used with the bridge at Tunyogmatolcs, but for dynamic measurements, a seven-channel FM tape-recorder of type TEAC was used.

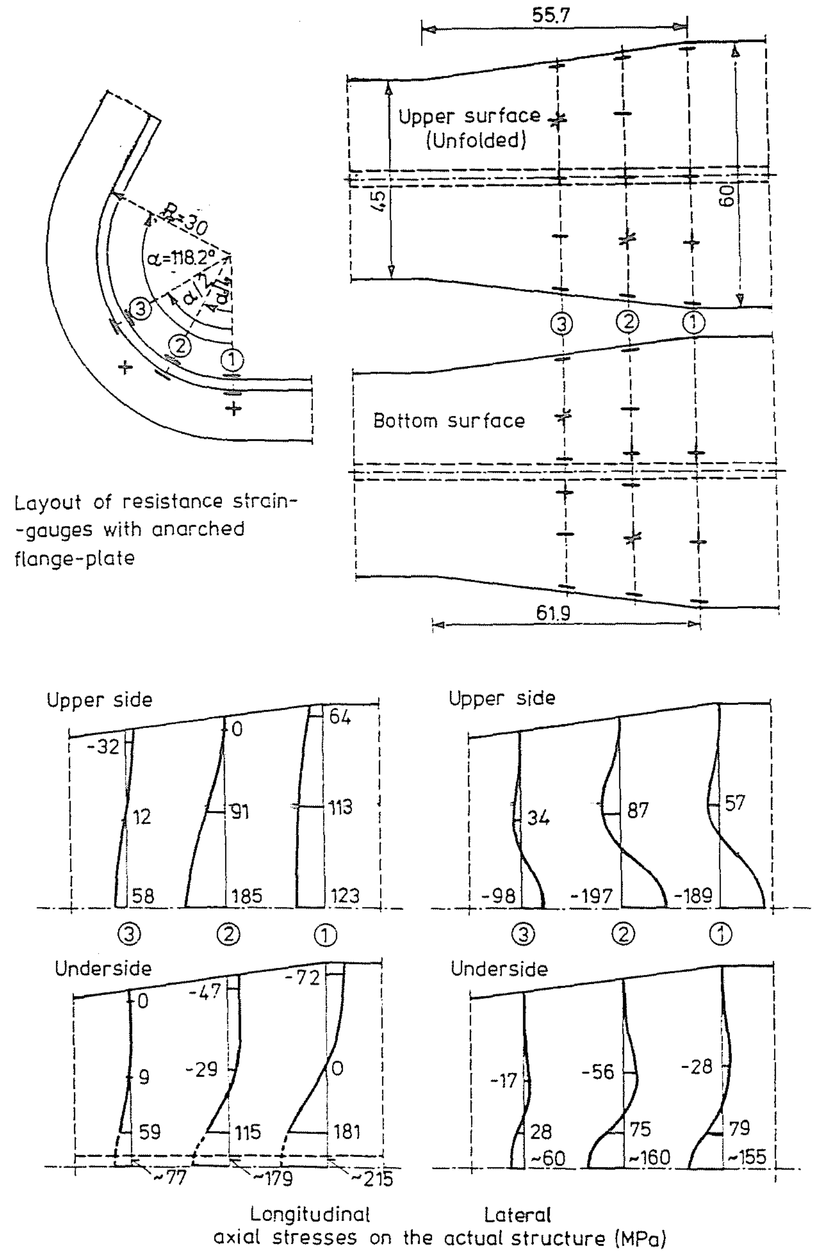

Fig. 10. Summary of the results gained by model experiments for testing one of the joints of the planned railway bridge at Simontornya having a layout similar to that of the bridge at Bánréve

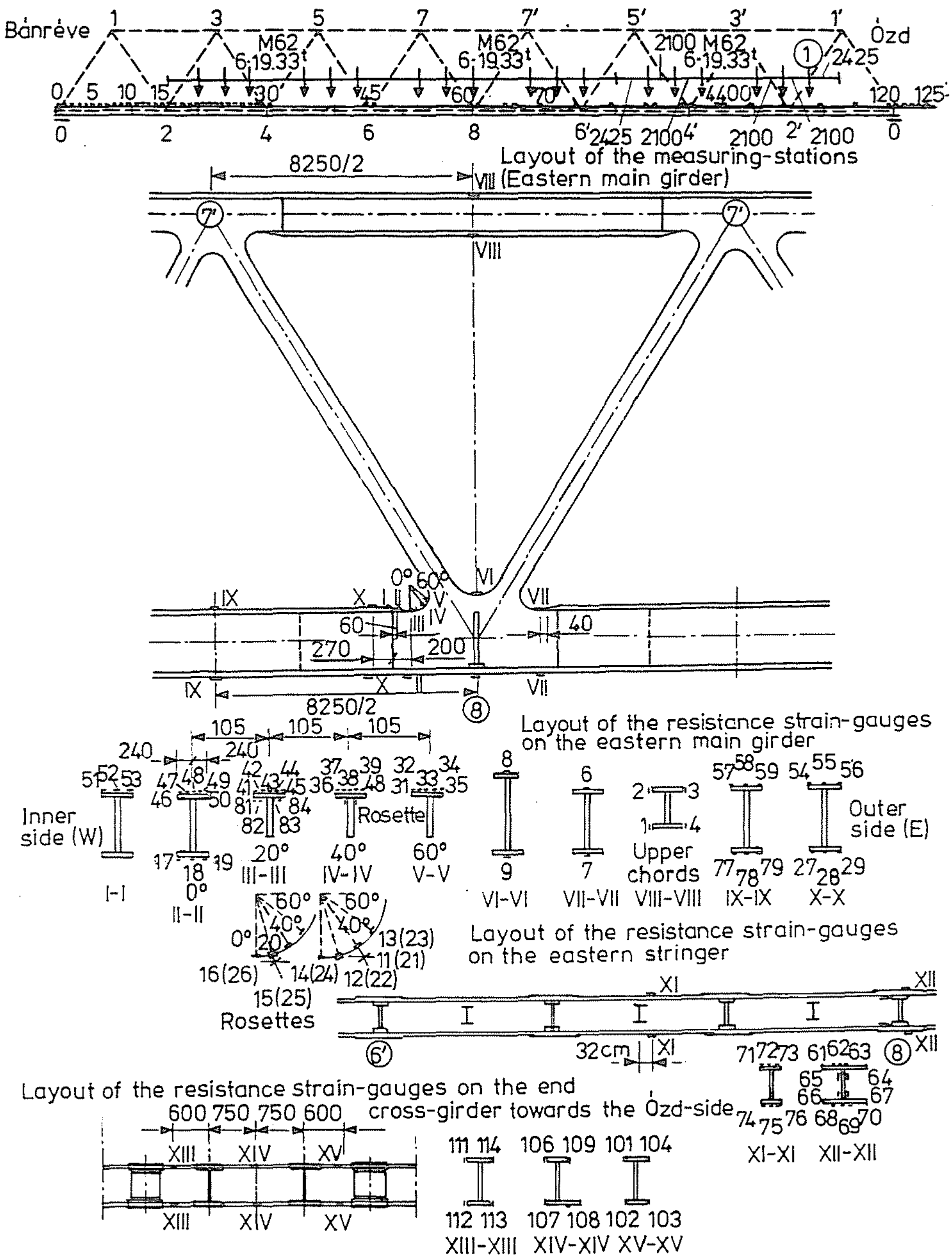

Fig. 11. Positioning of the measuring points during the loadtest of the bridge at Bánréve.

The up-to-date structure used with the bridge at Bánréve cannot be considered a simple one from measurement technique point of view, either. While with the truss girders of a traditional layout, the bars are in a uniaxial state of stress, the statical behaviour of this bridge owing to the sometimes drastic changes of the profiles, the arched flange plates, the relatively rigid joints, the bending of the chords caused by the intermediate cross girders, the considerable thickness (40 mm) at some places of the web plates and flange plates, the contribution of stringers, the rigid welded joints of the structure, etc. is only a faint reminder of the traditional force condition of the theoretical (jointed) trussed girders. The effect of the disturbing moment, the lateral bending of the arched flange plates, as well as that of the contribution between the main girder and the stringers seems almost impossible to be followed by exact calculation.

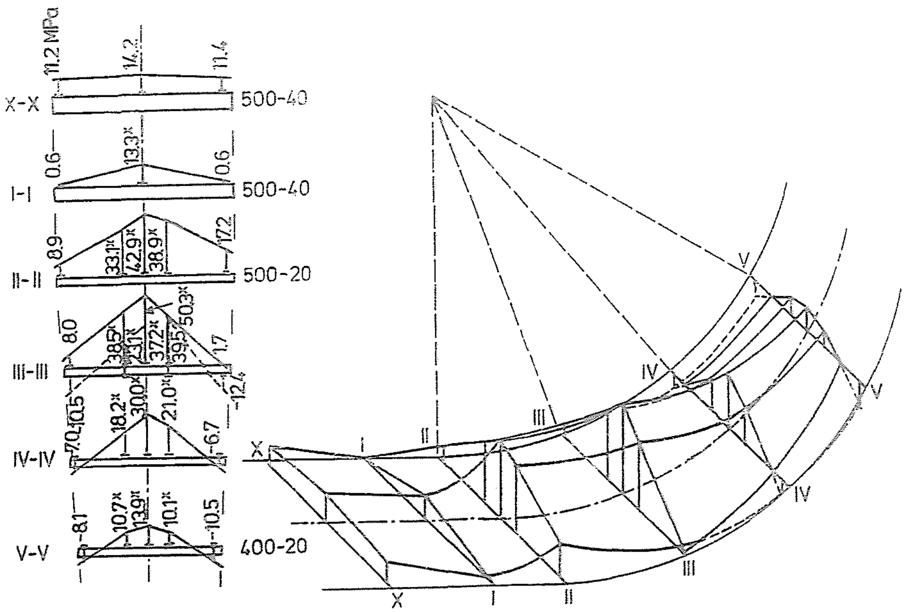

Fig. 12. Distribution of the stresses measured on the arched flange plate at joint No. 8

The most important experiences gained from the evaluation of the stresses, or internal forces, respectively, measured at the most unfavourable load-position, and those calculated for checking them were the following *(Table 2)*:

a) The normal stress calculated from the stresses measured on the edges of the flange-plates, in the middle of bars in the upper chord falls

Table 2

Measured element	Measured cross-position	Load	Gage position flange plate	σ_{aver} N/mm^2	σ_N N/mm^2	N_{meas} kN	N_{calc} kN	$\sigma_{M,upper}$ N/mm^2	M_{meas} kNm	M_{calc} kNm
upper chord 7–7'	VIII–VIII	Load I	upper	-51.5	-42.14	-2318	-2533	9.36	104.4	
			bottom	-32.78						
		Load II	upper	-51.15	-42.26	-2269		9.89	110.3	
			bottom	-31.38						
bottom cord 6–8	IX–IX	Load I	upper	10.2	24.3	1628	2458	14.1	306.9	
			bottom	38.4						
		Load II	upper	10.4	24.1	1616		13.7	298.2	
			bottom	37.8						
	X–X	Load I	upper	12.0	19.5	1306	2458	7.5	163.2	
			bottom	27.0						
		Load II	upper	12.0	19.42	1301		7.42	161.5	
			bottom	26.85						
	II–II	Load I	upper	27.6	26.07	1721	2458	1.53	24.1	
			bottom	24.9						
		Load II	upper	27.2	26.01	1717		1.19	18.7	
			bottom	25.1						
	VII–VII	Load I	upper	38.95	30.87	2037	2437	8.08	127.2	
			bottom	24.65						
		Load II	upper	38.25	30.87	2038		7.38	116.2	
			bottom	25.2						

Table 2

Measured element	Measured cross-position	Load	Gage position flange plate	σ_{aver} N/mm²	σ_N N/mm²	N_{meas} kN	N_{calc} kN	$\sigma_{M,upper}$ N/mm²	M_{meas} kNm	M_{calc} kNm
Stringer girder	middle 6–8	Load I	upper	10.88	21.86	385		10.98	32.89	26.48
			bottom	32.85						
		Load II	upper	12.07	21.1	346		9.03	27.04	
			bottom	30.12						
	support8	Load I	upper	27.12	12.83	382		14.29	-93.5	(-13.00)
			bottom	-1.47						
		Load II	upper	26.98	12.86	383		14.12	-92.4	
			bottom	-1.27						

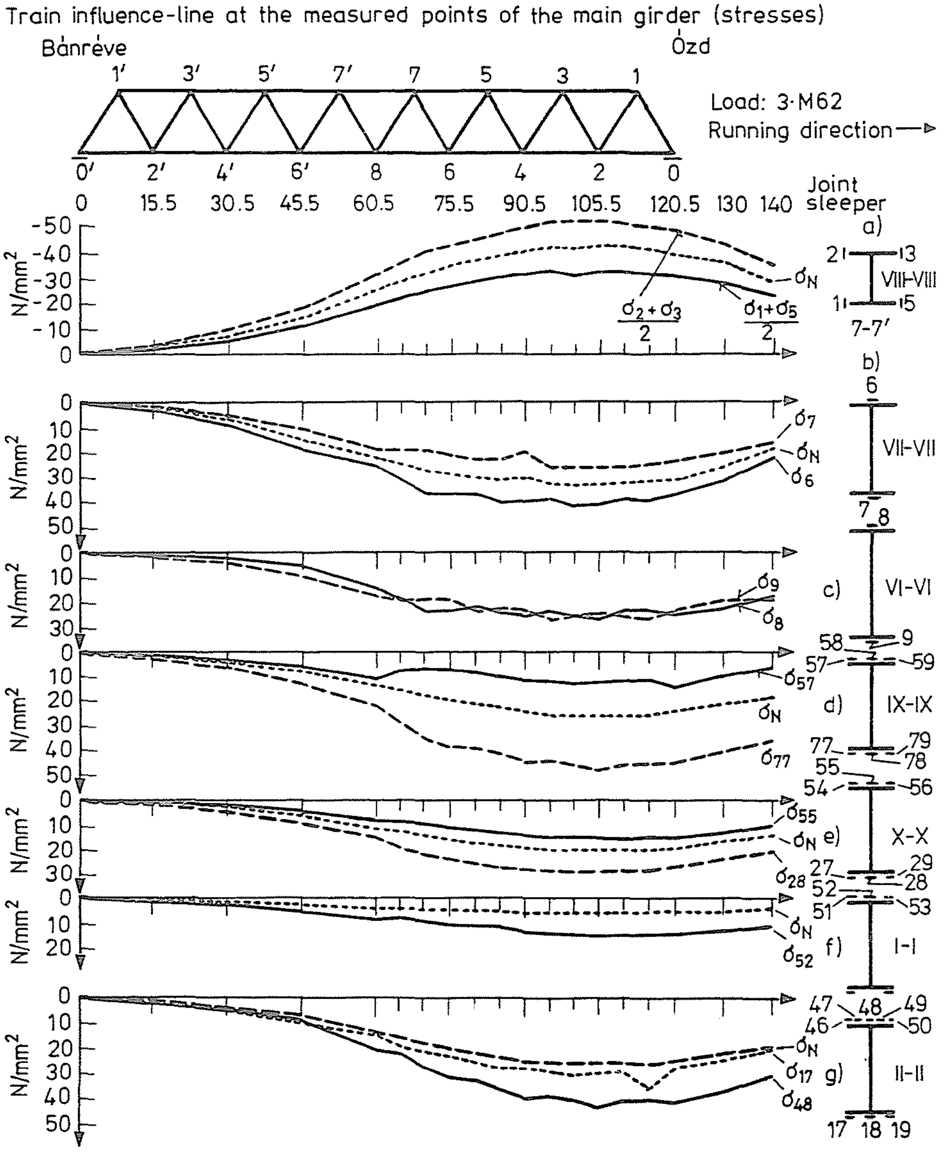

Fig. 13. Train influence lines of stresses for some points in characteristic cross-sections of the chords

behind the calculated one by about 10 %. Simultaneously with the normal force there is a considerable bending effect, too. The deviation

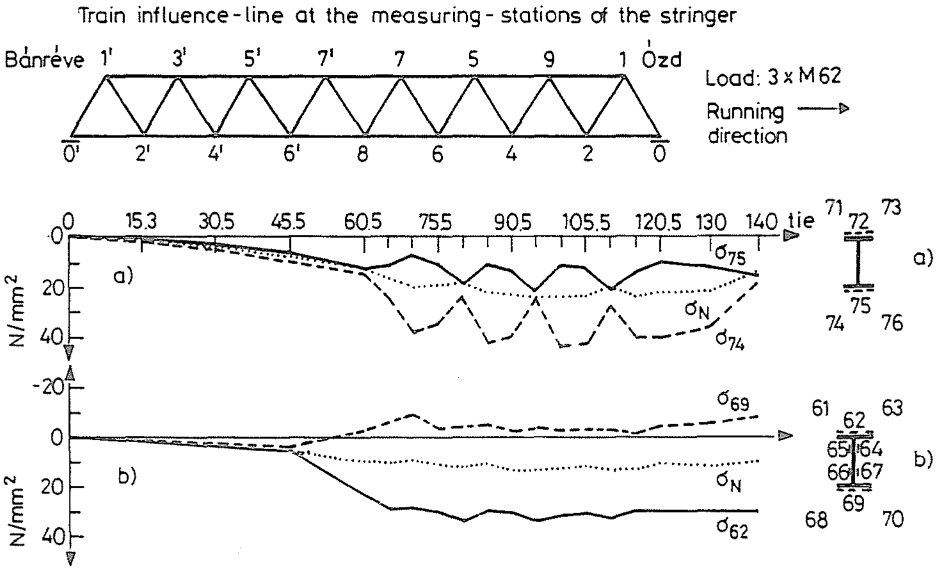

Fig. 14. Train influence lines of stresses for the characteristic points of the stringers

can be attributed to the deviation of the actual dimensions from the nominal ones, the non-uniform stress distribution along the cross-section (the stresses arisen in the flange-plate in the center line of the web plates are greater than the average stress), the contribution of the upper wind brace with the main girder.

b) The bar force calculated on the basis of the stress measured on the bottom chord falls short considerably of the calculated one across each cross-section, which can be explained by the contribution character of the main girder with the stringers, but the axial force calculated on the basis of the stresses measured on the stringers does not cover the shortage of the chord force, the drastic changes in the cross sectional areas of the web plate and flange plates especially those in the vicinity of changes exert a disturbing effect on stress distribution, the non-uniform stress distribution in the flange plates, the bottom wind-brace taking also part in the load-bearing of the bottom chord, in addition to that effect of the stringers.

c) The axial force and the bending moment calculated on the basis of the stresses measured on the stringers can be only hardly compared – due to the contribution of different loading elements – with the calculated results gained by help of influence lines.

d) Similarly, the comparison of the stresses measured and calculated at the end cross girder No.0 can be drawn only with much difficulty.

e) We tried to measure in detail the stress distribution in the arched plate functioning as an upper flange-plate of the bottom chord-bar No.6-8. The stresses measured at the points with tangents 0°, 20°, 40° and 60°, as well as in the place of the change in the thickness of the flange plate (from 40 mm down to 20 mm) are illustrated in *Fig. 12*. For the results to be evaluated, it should be noted that a considerable lateral bending will occur in the chords caused by the change in thickness and bending occurring with the arch of $R = 300$ mm. Since only the longitudinal strains were measured, the stress calculated on the basis of the measured strain can be considered correct only at the edges of the flange plate (free edge – uniaxial state of stress). At the points above the web plate, the strain will increase due to lateral bending. This increase – according to the measurements performed on the model of the bridge at Simontornya – amounts to 20-30 %, due to which the actual stress will be smaller by 20-30 % than that calculated on the basis of the unidirectional measurement.

f) From the measurement results obtained on the rosettes positioned on both sides of the web plate at a distance of about 20 mm from the web-to-flange weld in the section of a tangent of 20° and 40°, it is to be seen that in the section of a tangent of 20°, the directions of the principal stresses are nearly horizontal and vertical, in the section of a tangent of 40°, the direction of the principal tensile stress is about −15° , the principal stress in the '20°–section' is greater than that in the '40°–section'.

From among the train influence lines recorded with the use of three M 62-type locomotives coupled together, the following will be displayed (*Fig. 13*):

- upper chord bar No.7-7' of the main girder (section VIII-VIII),
- bottom chord bars No.6'-8 and 6-8, respectively (sections: I-I, II-II, VI-VI, VII-VII, IX-IX and X-X).

It can be seen clearly with each stress train influence line that the bars are subject to a considerable bending in addition to the axial force. In the bottom chord, bending is verified by the eccentricity due to the contribution effect of the floor beams as well as the bending effect caused by the intermediate cross girders. The ground of the bending force arisen in the upper chord is unknown.

In *Fig. 14*, the train influence lines of the stresses arisen in the middle of the section 6'-8 [$M_{max}^{(+)}$] and those arisen in the cross-section of the support at cross girder No. 8 [$M_{max}^{(--)}$] in the upper and bottom extreme fibres, as well as the influence line of the average stresses (normal components) are illustrated. From the comparison drawn between the two influence lines it can be seen that the normal stress at the support is smaller than in the middle of the length, however, due to the larger cross-sectional area at the support the normal forces in the two places are almost identical. The development of the moments reflects well the difference between the influence lines related to the middle of the length and to the support, respectively.

Dynamic Measurements

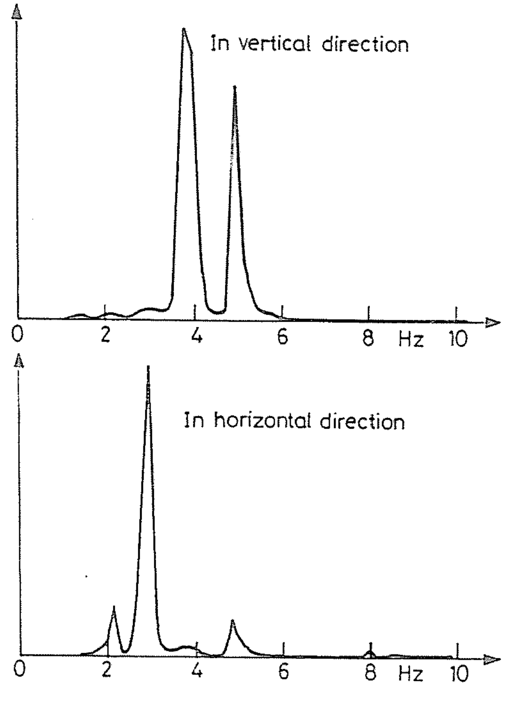

Fig. 15. Spectrum range of the vertical and horizontal natural frequencies

In the course of dynamic measurements,

the natural frequency,
the deflection of the bridge and
the changes in stresses

were investigated.

The results of the dynamic measurements this time, too, were recorded continuously and were processed later by a computer.

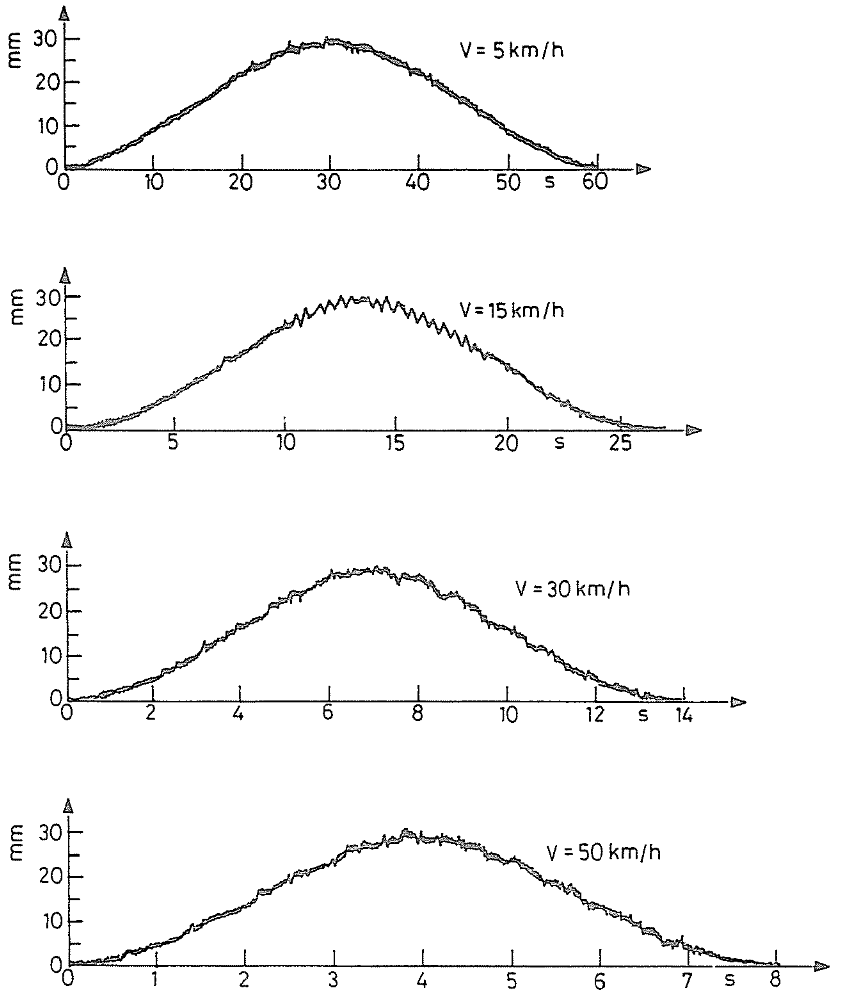

Fig. 16. Deflections by the effect of the loading train passing through at different speeds (downstream side of the bridge, Joint No.8, Load: 3×M62).

Two trains: 3 coupled and one single M62 locomotive served as dynamic load, passing through the bridge at different speeds.

The calculated first vertical bending natural frequency – using the simplified formula $f_0 = 5.6 \times e^{-1/2}$, where e is equal to the deflection due to the dead load, this case 2.43 cm – is 3.59 Hz. The measured first two vertical natural frequencies proved to be 3.7 and 4.8 Hz (*Fig. 15*), while the first horizontal bending natural frequency is 2.9 Hz.

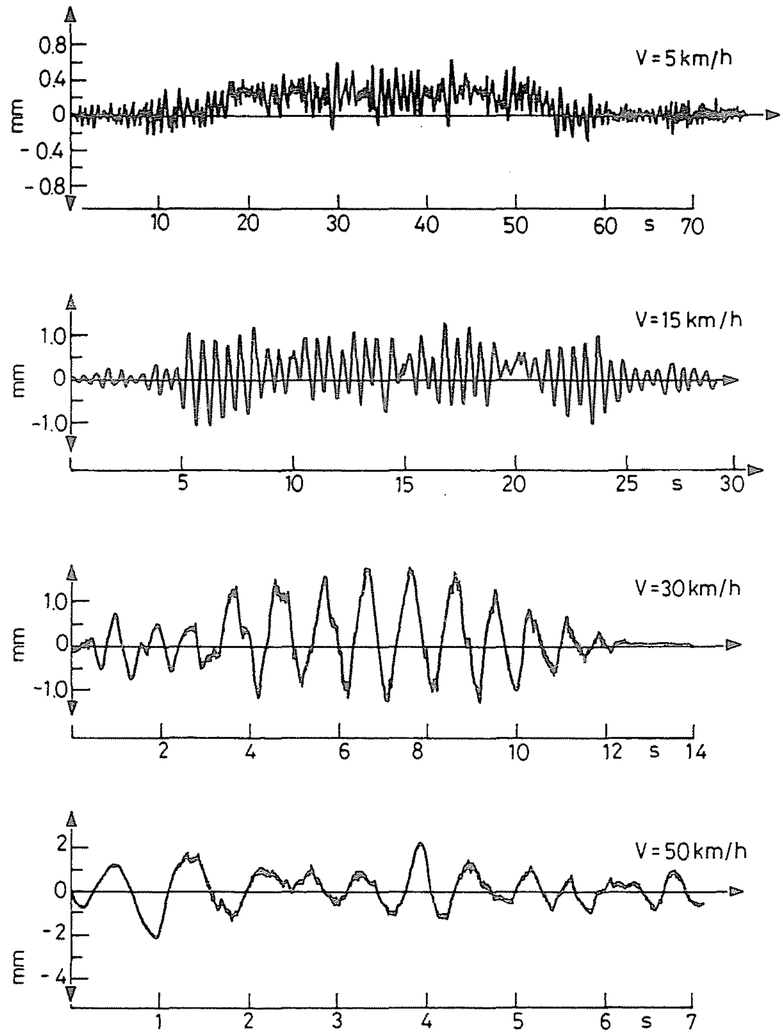

Fig. 17. Horizontal motion in lateral direction of the middle cross-section (Joint No.8.) by the effect of loading trains (3×M62) passing through the bridge at different speeds

The dynamic deflection of the main girder by the effect of 3 locomotives passing through at speeds of 5, 15, 30, and 50 km/h is illustrated in *Fig. 16.* The measured dynamic surplus in succession were: 1.6, 5.0, 4.2 and 4.2 %.

The lateral motion of the main girder at the above speed values can be seen in *Fig. 17.* The maximal values:

v [km/h]	5	15	30	50
	lateral movement [mm]			
3 locomotives	0.75	2.1	3.1	4.9
1 locomotive	1.1			1.9

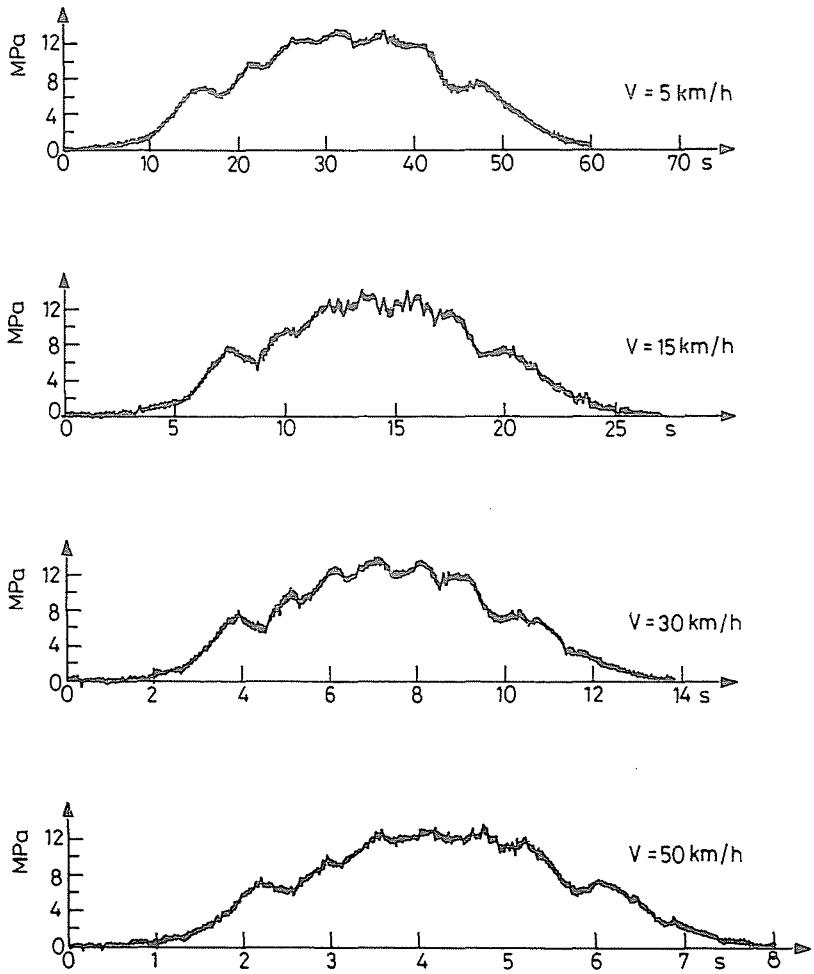

Fig. 18. Change of the stresses measured in measuring point No.55. positioned on the main girder under the influence of the loading train (3×M62) passing through at different speeds.

In *Fig. 18*, the stress time history, recorded by strain gage No.55 can be seen, as an example of the dynamic stress-measurements. Concluded from the measurement results, the dynamic surplus (%) was the following:

measuring	3 locomotives v(km/h)				1 locomotive v(km/h)	
point	5	15	30	50	5	50
48	1.2	4.8	5.0	4.9		
18	3.3	4.4	4.4	4.8		
58	3.6	5.1	6.9	7.6		
78	4.05	5.4	4.7	5.4		
28	2.6	3.9	3.6	5.3		
55	3.7	7.1	3.6	6.3	6.2	6.2
43	1.9	4.4	4.4	4.2	2.5	4.3

The UIC-ORE recommendation for the magnitude of the dynamic surplus will be given by relationship:

$$\phi = 0.65 \cdot K/(1 - K - K^2),$$

where K can be calculated by the formula
if v =speed [m/sec]
L =span [m]
f =natural frequency [Hz]

$$K = v/(2 \cdot L \cdot f).$$

The UIC-ORE gives also the standard deviation for the formula recommended, as follows

$$s = 0.025[1 + 18 \cdot K/(1 - K - K^2)].$$

The dynamic surplus occurring with a probability of 95.7 % will be:

$$\phi_{96} = \phi \pm 2 \cdot s,$$

which involves 9.4 % for the main girder of the bridge examined at a speed of 50 km/h, a greater value than any obtained by measurement.

According to the Railway Bridge Standard of 1951, the dynamic factor for the bridge at Bánréve

$$\mu = 1.1 + 15/(L + 21) = 1.27,$$

which provides a value even higher than that contained in the UIC-ORE recommendation.

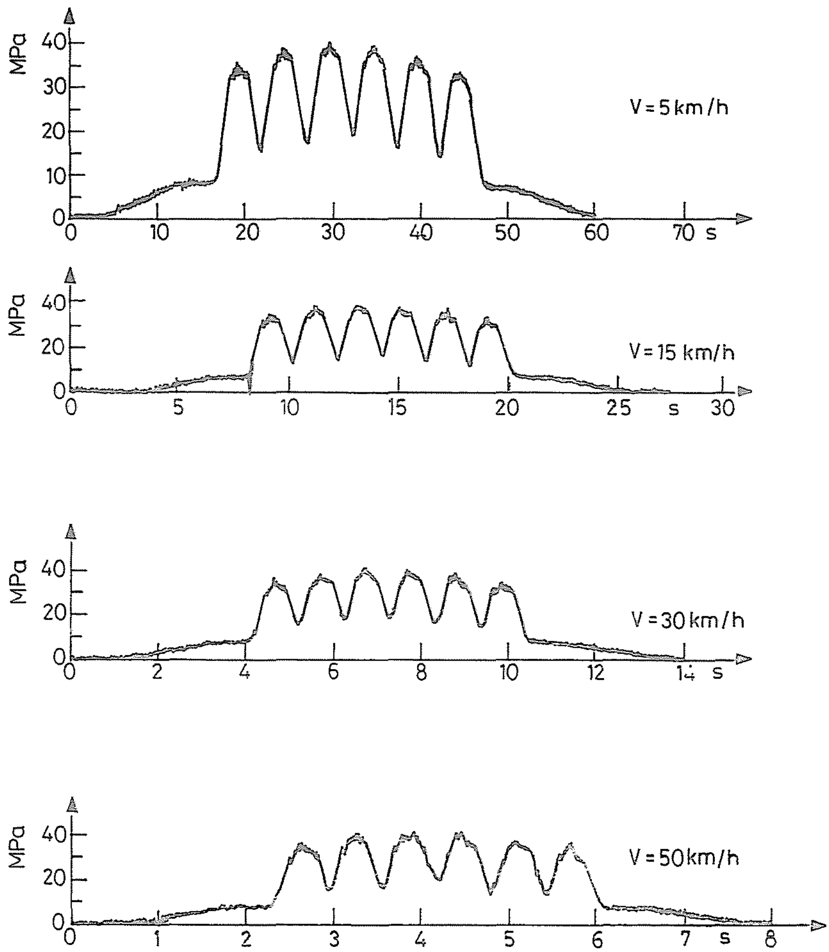

Fig. 19. Change of stresses in the stringer in measuring point No.75, under the influence of the loading trains (3×M62) passing through

measuring	3 locomotives v(km/h)				1 locomotive v(km/h)	
point	5	15	30	50	5	50
62	2.8	3.6	4.3	5.5	4.8	7.4
72	5.5	5.5	5.5	8.1	8.7	23.0*
75	2.7	5.0	5.0	5.0	2.0	7.1

As for the dynamic investigations related to the stringers, an illustration is given in *Fig. 19* and *Fig. 20*, where data recorded by a strain gage, positioned in a stringer (midspan, bottom chord) are presented, for the cases of different-speed 3 locomotive and 1 locomotive passes. After the evaluation of records of several corresponding measuring elements, the maximal dynamic surplus proved to be:

The dynamic surplus indicated by * was measured at a stress level well below the most unfavourable one.

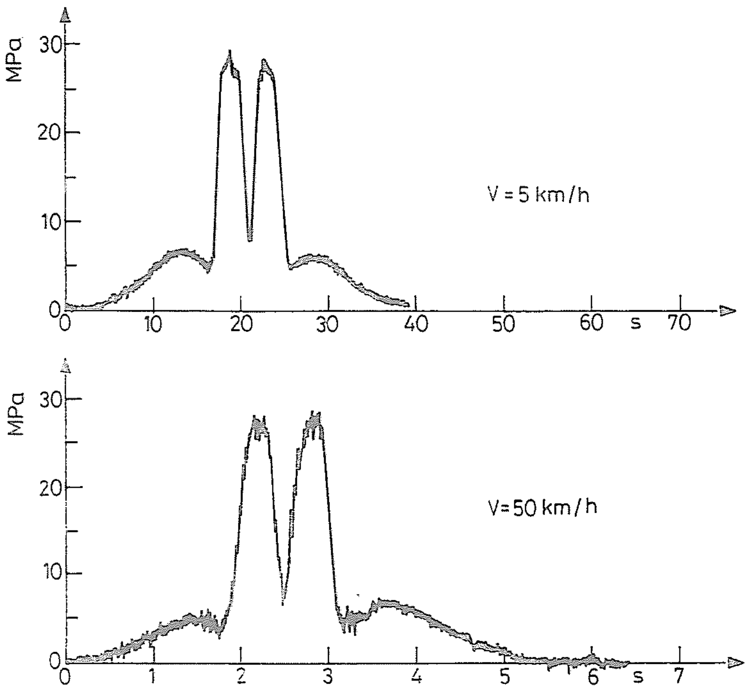

Fig. 20. Change of stresses in the stringer in measuring point No.75, under the influence of a single loading M62-type locomotive passing through

The UIC-ORE recommendation calculates the dynamic factor for stringers using the formulae:

$$\phi = 0.033 \cdot v,$$

$$s = 0.066(1 + 0.01 \cdot v).$$

The calculated dynamic surplus , with a probability of 95.7 % and supposing 50 km/h speed, will be 27.1 %, which is greater than any value obtained by measurement.

From the analysis of the dynamic measurements with respect to fatigue, the following important conclusions can be reached:

In the case of a train consisting of 3 M62 locomotives nearly totalling the full length of the bridge when passing through it

- each train-pass involves one maximum (i.e. one fatigue-cycle) for the mains, similarly, each pass involves one maximum for the stringers at the cross-section at the supports (M-max), however, in case of stringer midspan stresses, each group of axles (which consists of 3 axles with the M62 locomotives) causes one maximum (M+max), the stress-amplitudes on the cross-girders are small due to their dense layout.

Address:

Dr Antal SZITTNER
Dr Miklós KÁLLÓ
Dr László KÖRÖNDI
Department of Steel Structures
Technical University, H-1521 Budapest,
Hungary